

Evidence for Differential Roles for NKG2D Receptor Signaling in Innate Host Defense against Coronavirus-Induced Neurological and Liver Disease[∇]

Kevin B. Walsh,¹ Melissa B. Lodoen,³ Robert A. Edwards,^{2,4}
Lewis L. Lanier,³ and Thomas E. Lane^{1,2*}

Department of Molecular Biology & Biochemistry¹ and Center for Immunology,² University of California, Irvine, California 92697; Department of Microbiology & Immunology and Cancer Research Institute, University of California, San Francisco, California 94143³; and Department of Pathology & Laboratory Medicine, School of Medicine, University of California, Irvine, California 92697⁴

Received 13 September 2007/Accepted 13 December 2007

Infection of SCID mice with a recombinant murine coronavirus (mouse hepatitis virus [MHV]) expressing the T-cell chemoattractant CXC chemokine ligand 10 (CXCL10) resulted in increased survival and reduced viral burden within the brain and liver compared to those of mice infected with an isogenic control virus (MHV), supporting an important role for CXCL10 in innate immune responses following viral infection. Enhanced protection in MHV-CXCL10-infected mice correlated with increased gamma interferon (IFN- γ) production by infiltrating natural killer (NK) cells within the brain and reduced liver pathology. To explore the underlying mechanisms associated with protection from disease in MHV-CXCL10-infected mice, the functional contributions of the NK cell-activating receptor NKG2D in host defense were examined. The administration of an NKG2D-blocking antibody to MHV-CXCL10-infected mice did not reduce survival, dampen IFN- γ production in the brain, or affect liver pathology. However, NKG2D neutralization increased viral titers within the liver, suggesting a protective role for NKG2D signaling in this organ. These data indicate that (i) CXCL10 enhances innate immune responses, resulting in protection from MHV-induced neurological and liver disease; (ii) elevated NK cell IFN- γ expression in the brain of MHV-CXCL10-infected mice occurs independently of NKG2D; and (iii) NKG2D signaling promotes antiviral activity within the livers of MHV-infected mice that is not dependent on IFN- γ and tumor necrosis factor alpha secretion.

Viral infection often results in a rapid and coordinated immune response, culminating in the control of viral replication and limited pathology. Although numerous signaling pathways are elicited early following viral infection, chemokines are rapidly expressed in response to infection and represent a potentially important component of the innate immune response (6, 10, 19, 20, 39, 40). In support of this possibility, we previously demonstrated that the CXC chemokine ligand 10 (CXCL10) is detected within 24 h following intracranial (i.c.) instillation of neuroadapted strains of the murine coronavirus mouse hepatitis virus (MHV), suggesting an important role for CXCL10 in the innate immune response (38). CXCL10 is a potent chemoattractant for both activated T lymphocytes and natural killer (NK) cells by signaling through the receptor CXCR3, which is expressed on the surface of these cells (26, 32, 36, 37, 42). Indeed, infection of *Rag1*^{-/-} mice with a recombinant MHV that generates functional CXCL10 (MHV-CXCL10) results in protection from disease that correlated with increased NK cell infiltration into the central nervous system (CNS), accompanied by a reduction in viral titers within the brain (38). Treatment of MHV-CXCL10-infected mice with blocking CXCL10 antibody or depletion of NK cells enhanced viral

recovery from the CNS (38). The NK cell-mediated protection from disease correlated with elevated levels of gamma interferon (IFN- γ) within the brain, suggesting that CXCL10 signaling contributed to defense by attracting activated NK cells into the CNS.

Antiviral effector properties of NK cells can be evoked through various signaling pathways. NKG2D is one such activating receptor expressed on NK cells. In mice, ligands for the NKG2D receptor include the retinoic acid early inducible-1 (RAE-1) proteins (RAE-1 α , RAE-1 β , RAE-1 γ , RAE-1 δ , and RAE-1 ϵ), minor histocompatibility antigen H60, and murine UL16-binding protein-like transcript-1 (MULT1) glycoprotein. These ligands are expressed by cells undergoing cellular stress, such as viral infection, DNA damage, or transformation (2, 4, 5, 7–9, 12, 24). The ligation of NKG2D by these molecules enhances NK cell cytolytic activity, cytokine production, and chemokine secretion, thereby providing defense against tumors and viral infection (2, 5, 8, 12, 24). Highlighting the importance of NKG2D in antiviral host defense are studies demonstrating that mouse cytomegalovirus (MCMV) has successfully evaded recognition by the NKG2D receptor by its expression of several viral proteins that inhibit the expression of the NKG2D ligands in MCMV-infected cells (18, 23–25).

The current study was undertaken to further define the mechanisms by which CXCL10 contributes to NK cell activation and host defense following viral infection. Specifically, the data presented extend our previous studies by examining defense in response to viral infection of both the brain and liver

* Corresponding author. Mailing address: Department of Molecular Biology & Biochemistry, 3205 McGaugh Hall, University of California, Irvine, Irvine, CA 92697-3900. Phone: (949) 824-5878. Fax: (949) 824-8551. E-mail: tlane@uci.edu.

[∇] Published ahead of print on 19 December 2007.

as well as determining whether NKG2D participates in CXCL10-mediated protection within the context of the innate immune response. The data presented indicate that NKG2D is not essential in the protection provided by CXCL10 within the brain following MHV-CXCL10 infection of SCID mice. In contrast, NKG2D signaling in the liver reduces the MHV-CXCL10 viral burden without affecting pathology. These studies demonstrate that NK cell protection afforded by CXCL10 expression differs depending on the organ and is partially NKG2D dependent in the liver.

MATERIALS AND METHODS

Mice and reagents. The generation of MHV-CXCL10 and control MHV has been previously described (38). Both viruses originally were derived from the parental MHV-A59 strain, which is capable of replicating in the brain and liver following i.c. instillation into susceptible mice (22). SCID mice (BALB/c, H-2^d background) were purchased from the National Cancer Institute. Mice were anesthetized by intraperitoneal (i.p.) injection with a 150- μ l mixture of ketamine hydrochloride (Ketaject; 100 μ g/ml; Phoenix, St. Joseph, MO) and xylazine hydrochloride (1.1 mg/ml; ICN Biomedical, Aurora, OH) in Hanks' balanced salt solution (HBSS). Anesthetized mice were injected i.c. with 1,000 PFU of MHV-CXCL10 or MHV suspended in 30 μ l of sterile HBSS. Sham-infected animals were injected with 30 μ l of sterile HBSS alone. Mice were sacrificed and perfused with sterile phosphate-buffered saline (PBS) on days 3 and 5 postinfection (p.i.), at which point brains and livers were removed for the determination of virus titers on a susceptible astrocytoma cell line (DBT) (14, 20). The production of CX5 (a neutralizing, nondepleting rat anti-mouse NKG2D) monoclonal antibody (MAb) was performed as previously described, and saturated ammonium sulfate precipitation was performed to purify the antibody from the ascites fluid (29). Small-molecular-weight proteins were removed by dialysis, and the antibody concentration was determined using a rat immunoglobulin G (IgG)-specific enzyme-linked immunosorbent assay (ELISA). MHV-CXCL10-infected SCID mice were treated i.p. 2 days before infection and 3 and 7 days p.i. with 100 μ g of CX5 or control rat IgG (Sigma-Aldrich, St. Louis, MO) suspended in 300 μ l of 1 \times HBSS (Mediatech Inc., Herndon, VA).

Quantitative real-time PCR. Total RNA was extracted from homogenized liver and brain samples by using TRIzol reagent (Invitrogen, Carlsbad, CA), DNase treated, and purified via phenol-chloroform extraction. RNA was reverse transcribed by using a Moloney murine leukemia virus reverse transcriptase kit (Invitrogen, Carlsbad, CA) and random hexamers (Promega, Madison, WI). Quantitative real-time PCR was performed using a Bio-Rad (Hercules, CA) iCycler instrument according to the manufacturer's instructions. The real-time Taqman analysis for NKG2D ligand transcripts was performed using previously described primers and probes (13, 28, 29). Probes were purchased from Integrated DNA Technologies (Coralville, IA), and primers were purchased from Invitrogen (Carlsbad, CA). Bio-Rad (Hercules, CA) iQ Supermix was used for the reactions. The cycling conditions used for the quantitative PCR were the following: 95°C for 4 min, followed by 40 cycles at 95°C for 30 s and at 58°C for 30 s. Data were analyzed by using the Bio-Rad (Hercules, CA) iCycler iQ version 3.0a software. Data were quantitated by using the relative expression software tool, version 2 (31).

Pathology and immunohistochemistry. Brains and livers were removed at day 5 p.i. and placed in 5 ml of Formal-Fixx (ThermoShandon, Pittsburgh, PA) overnight at room temperature, after which portions of tissue were embedded in paraffin. Hematoxylin and eosin staining was performed on liver sections to reveal differences in inflammation. For each specimen, livers were evaluated for the degree of disease activity present. Lesions in each sample were scored according to a semiquantitative scoring system based on the evaluation of five parameters that were each graded on a 0 to 3 scale (0, none; 1, mild; 2, moderate; and 3, severe) (41). The parameters that were scored included the degree of portal inflammation, the degree of sinusoidal inflammation, the presence and severity of endothelialitis, the degree of hepatocyte necrosis, and the presence of reactive hepatocytomegaly. The distribution of viral antigen was determined by immunoperoxidase staining (Vectastain-ABC kit; Vector Laboratories, Burlingame, CA) using the anti-MHV MAb J.3.3, which is specific for the carboxyl terminus of the viral nucleocapsid protein, as a primary antibody and horse anti-mouse IgG as the secondary antibody (Vector Laboratories, Burlingame, CA) (3). Serum alanine aminotransferase (sALT) concentrations were determined by using Infinity ALT (GPT) liquid stable reagent (Thermo, Noble Park, Victoria, Australia) according to the manufacturer's specifications.

Mononuclear cell isolation and flow cytometry. Immunophenotyping of the cellular infiltrate present within brains and livers of infected mice was accomplished by homogenizing isolated tissue and generating a single-cell suspension for analysis by flow cytometry, as previously described (20). Fc receptors were blocked by using 2.5 μ g/ml of anti-mouse CD16/CD32 MAb (2.4G2) (Pharmin-gen, San Diego, CA) in staining buffer (1 \times PBS, 0.1 g/liter bovine serum albumin). Allophycocyanin (APC)-conjugated anti-CD49b MAb DX5 (Miltenyi Biotech, Bergisch Gladbach, Germany), fluorescein isothiocyanate-conjugated Armenian hamster anti-mouse CD3e (BD Pharmingen, San Diego, CA), and phycoerythrin (PE)-conjugated rat anti-mouse NKG2D MAb CX5 (eBioscience, San Diego, CA) were used to detect NKG2D-positive NK cells. As controls, isotype-matched APC-, fluorescein isothiocyanate-, and PE-conjugated MAbs were used. Cells were incubated with MAbs for 30 min at 4°C, washed, and analyzed on a FACStar (BD Biosciences, Mountain View, CA). Data are presented as the percentage and total number of positive cells within the gated population. NKG2D receptor surface expression was determined by incubating cells with a biotin-conjugated NKG2D-specific antibody, MI-6 (16) (eBioscience, San Diego, CA), at 2.5 μ g/ml for 30 min at 4°C. Cells were washed and incubated with PE-conjugated streptavidin (eBioscience, San Diego, CA) at 1 μ g/ml for 30 min at 4°C. Cells were analyzed as described above, and data are presented as representative histograms with mean fluorescent intensities (MFI) indicated.

Intracellular IFN- γ and granzyme B staining. Brain and liver single-cell suspensions were obtained as described above, and NK cells were stained using APC-conjugated anti-NKG2D MAb DX5 (eBioscience, San Diego, CA). The cells then were fixed and permeabilized by using a BD cytofix/cytoperm plus kit (BD Pharmingen, San Diego, CA). Cells were stained for intracellular IFN- γ or granzyme B for 30 min at 4°C by using a PE-conjugated rat anti-mouse IFN- γ (BD Pharmingen, San Diego, CA) or mouse anti-human granzyme B antibody (Invitrogen, Burlingame, CA). Nonreactive PE-conjugated rat IgG1 (BD Pharmingen, San Diego, CA) or mouse IgG1 antibody (Invitrogen, Burlingame, CA) was used as an isotype-matched Ig control. Samples were analyzed on a FACStar (BD Biosciences, San Jose, CA).

ELISA. Livers were removed and homogenized in 2 ml PBS supplemented with Complete Mini, EDTA-free protease inhibitor cocktail (two tablets in 14 ml PBS) (Roche, Mannheim, Germany). Supernatants were clarified by centrifugation. ELISAs were performed by using the DuoSet mouse IFN- γ ELISA kit (R&D Systems, Minneapolis, MN) and the mouse tumor necrosis factor alpha (TNF- α) ELISA ready-set-go kit (eBioscience, San Diego, CA), as specified by the manufacturer, to determine the amounts of IFN- γ and TNF- α , respectively.

Statistical analysis. Statistically significant differences between groups of mice were determined by the *t* test using Sigma-Stat 2.0 software (Jandel, Chicago, IL), and *P* values of 0.05 or less were considered significant. Statistical analysis on survival was performed using the Fisher's exact test, and a two-tailed *P* value of ≤ 0.05 was considered significant (1, 21).

RESULTS

Infection with MHV-CXCL10 increases survival of SCID mice. To evaluate the role of CXCL10 in promoting innate host defense following infection with a murine coronavirus, a recombinant MHV was constructed with the coding sequence for CXCL10 inserted into open reading frame 4 within the viral genome (38). The parental strain of MHV used to construct MHV-CXCL10 and the isogenic control virus are capable of infecting and replicating within the liver following i.c. infection (22). Therefore, infection with the recombinant MHV-CXCL10 allows for the determination of the role of this chemokine in antiviral defense following infection of both the brain and liver. Instillation of MHV-CXCL10 into the CNS of SCID mice (BALB/c background) resulted in increased survival compared to that of mice infected with the isogenic control virus, MHV. These results are consistent with those of earlier studies, demonstrating that MHV-CXCL10 infection of *Rag1*^{-/-} mice on the C57BL/6 background also results in enhanced protection from disease compared to that of mice infected with an isogenic control virus (38). Infection with MHV resulted in mortality at day 5 p.i., with 100% of mice deceased by day 7 p.i. (Fig. 1A). In contrast, infection with MHV-

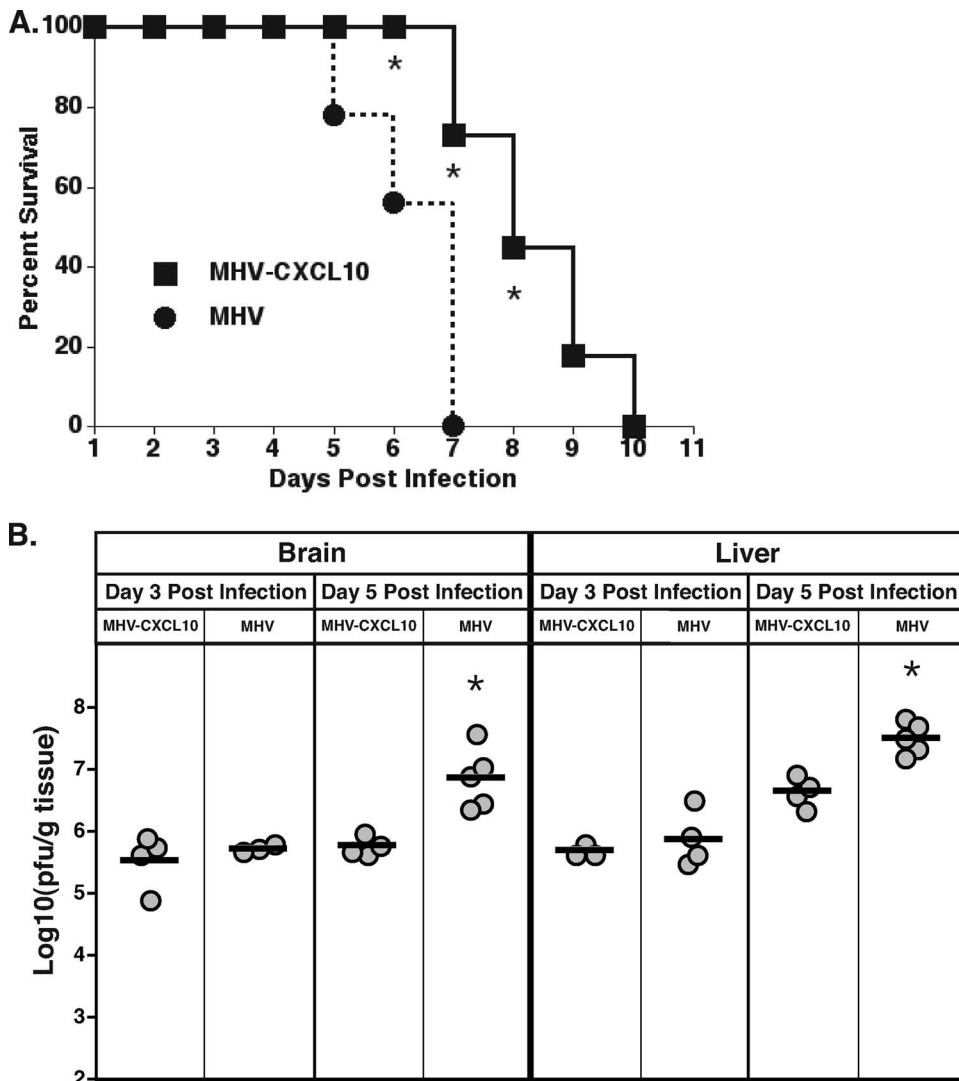


FIG. 1. Enhanced survival and reduced viral titers in mice infected with MHV-CXCL10. (A) Infection of SCID mice with MHV resulted in death beginning at day 5 p.i., with 100% mortality by day 7 p.i. In contrast, death in MHV-CXCL10-infected SCID mice was first observed at day 7 p.i., with 100% mortality by day 10 p.i. There was a significant (*, $P \leq 0.05$) increase in the survival of MHV-CXCL10-infected mice at days 6, 7, and 8 p.i. compared to that of MHV-infected mice. Data are representative of two combined experiments with a minimum of four mice per group for each experiment. (B) Viral titers were similar in the brains and livers of MHV-CXCL10- and MHV-infected mice at day 3 p.i. By day 5 p.i., MHV-infected brains and livers had significantly (*, $P \leq 0.05$) increased viral titers compared to those of tissues isolated from MHV-CXCL10-infected mice. Circles represent individual mice, and the averages per group are displayed as solid black bars. The assessment of viral burden was performed twice with no fewer than three mice per group at each time point.

CXCL10 prolonged survival, with the onset of death beginning at day 7 p.i. and 100% mortality being reached by day 10 p.i. (Fig. 1A). Viral plaque assays of both brains and livers from infected animals revealed comparable viral titers in MHV-CXCL10- and MHV-infected mice at day 3 p.i. (Fig. 1B). By day 5 p.i., viral titers in both tissues were significantly ($P \leq 0.05$) greater in MHV-infected mice than in MHV-CXCL10-infected mice (Fig. 1B). We have previously demonstrated that the enhanced survival and lower viral titers in mice infected with MHV-CXCL10 are NK cell dependent, as the depletion of NK cells eliminates these protective effects (38). Further, there were no apparent differences in cellular tropism between MHV-CXCL10 and the isogenic control virus following CNS

infection with glial cells (e.g., astrocytes, microglia, and oligodendrocytes containing viral antigen) (not shown).

The examination of livers at day 5 p.i. revealed that liver sections from MHV- and MHV-CXCL10-infected mice had considerable tissue damage compared to livers from uninfected mice (Fig. 2F). A diffuse interface hepatitis was present, centered on the portal tracts (Fig. 2A to D). As indicated above, necrotic periportal hepatocytes mixed with a predominantly neutrophilic infiltrate were detected (Fig. 2B and D). In many cases, the portal vessels were obscured or obliterated. The surrounding viable hepatocytes appeared reactive, with various degrees of anisonucleosis and multinucleation. A lesser mononuclear infiltrate occasionally was present within the surrounding sinusoids. In gen-

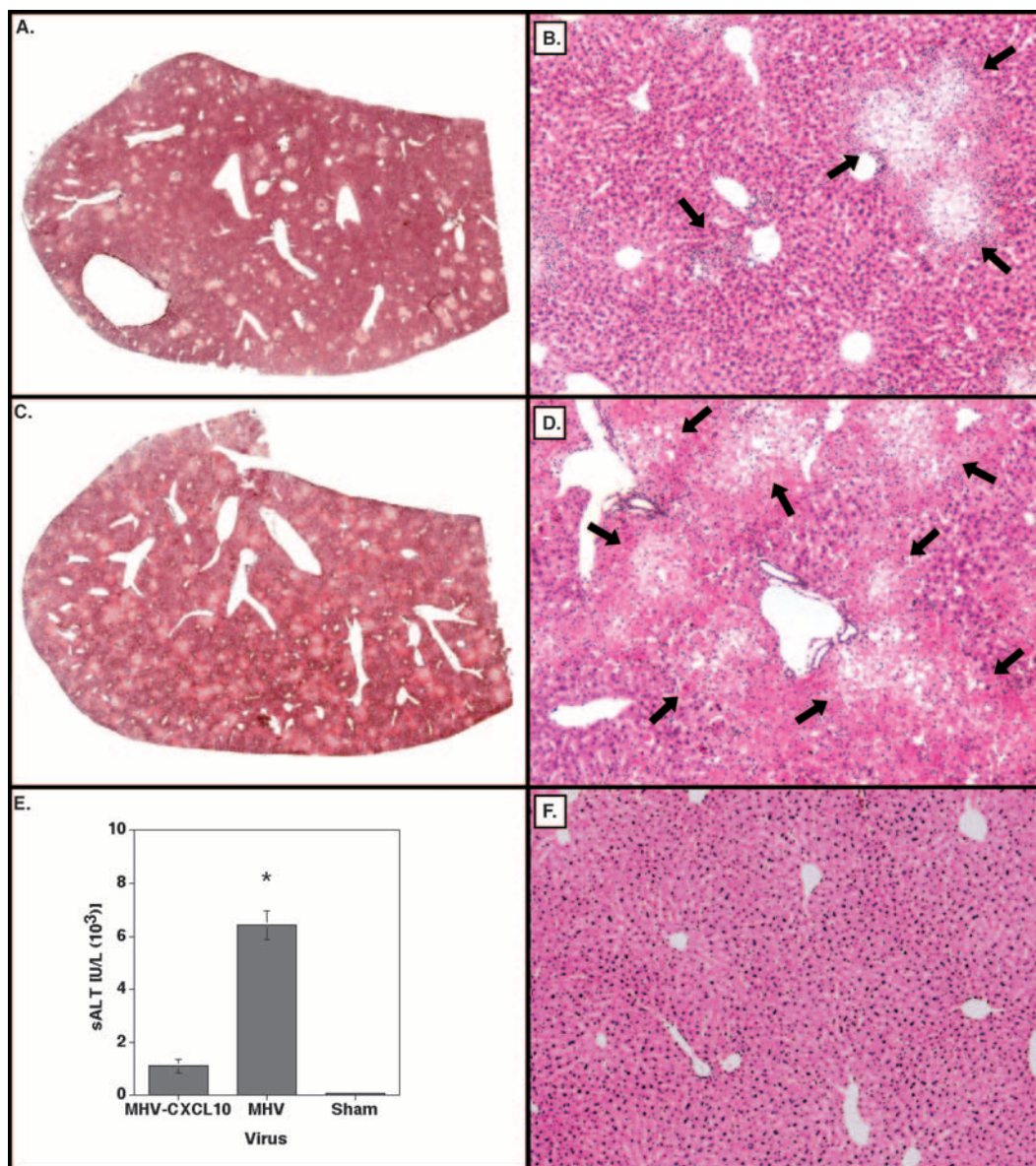


FIG. 2. Severity of viral hepatitis was reduced in mice infected with MHV-CXCL10. Sections of livers from MHV- and MHV-CXCL10-infected mice revealed considerable tissue damage compared to tissue of sham-infected control livers. A diffuse interface hepatitis was present, centered on the portal tracts with concentric rings of necrotic hepatocytes mixed with a predominantly neutrophilic infiltrate. Hepatitis was present in both MHV-CXCL10-infected (A and B) and MHV-infected (C and D) mice at day 5 p.i. However, mice infected with MHV (C and D) had more severe hepatitis than MHV-CXCL10-infected mice (A and B). (E) In correlation with these findings, MHV-infected mice exhibited significantly ($*$, $P \leq 0.01$) increased levels of sALT compared to those of MHV-CXCL10-infected mice, further supporting the finding of increased liver disease in MHV-infected mice at day 5 p.i. sALT data are representative of four separate experiments and no fewer than two mice per group. (F) Representative liver section from a sham-infected mouse. Histology was performed for two separate experiments, with two mice per group and a minimum of six sections per mouse examined. Arrows indicate areas of inflammation and necrosis. Panels A and C, $\times 2$ magnification; panels B, D, and F, $\times 40$ magnification.

eral, the degree of tissue damage was greater in the livers from mice that received control MHV (10.7 ± 1.0 ; $n = 3$) (Fig. 2C and D) than in the livers of mice that received MHV-CXCL10 (7.5 ± 1.0 ; $n = 3$) (Fig. 2A and B). In addition, MHV-infected mice exhibited significantly increased ($P \leq 0.01$) levels of sALT within the blood compared to those of MHV-CXCL10-infected mice, further supporting the presence of increased liver disease in MHV-infected mice (Fig. 2E).

NK cell infiltration and IFN- γ expression. Immunophenotyping of the cellular infiltrate revealed comparable total numbers of NK cells (determined by DX5 expression) infiltrating into the brain at days 3 and 5 p.i. between experimental groups (Fig. 3A). In the liver, NK cell numbers were equivalent in MHV-CXCL10- and MHV-infected mice at day 3 p.i. (Fig. 3D), yet MHV-infected mice exhibited increased numbers of NK cells within the livers at day 5 p.i. compared to those of MHV-CXCL10-infected mice

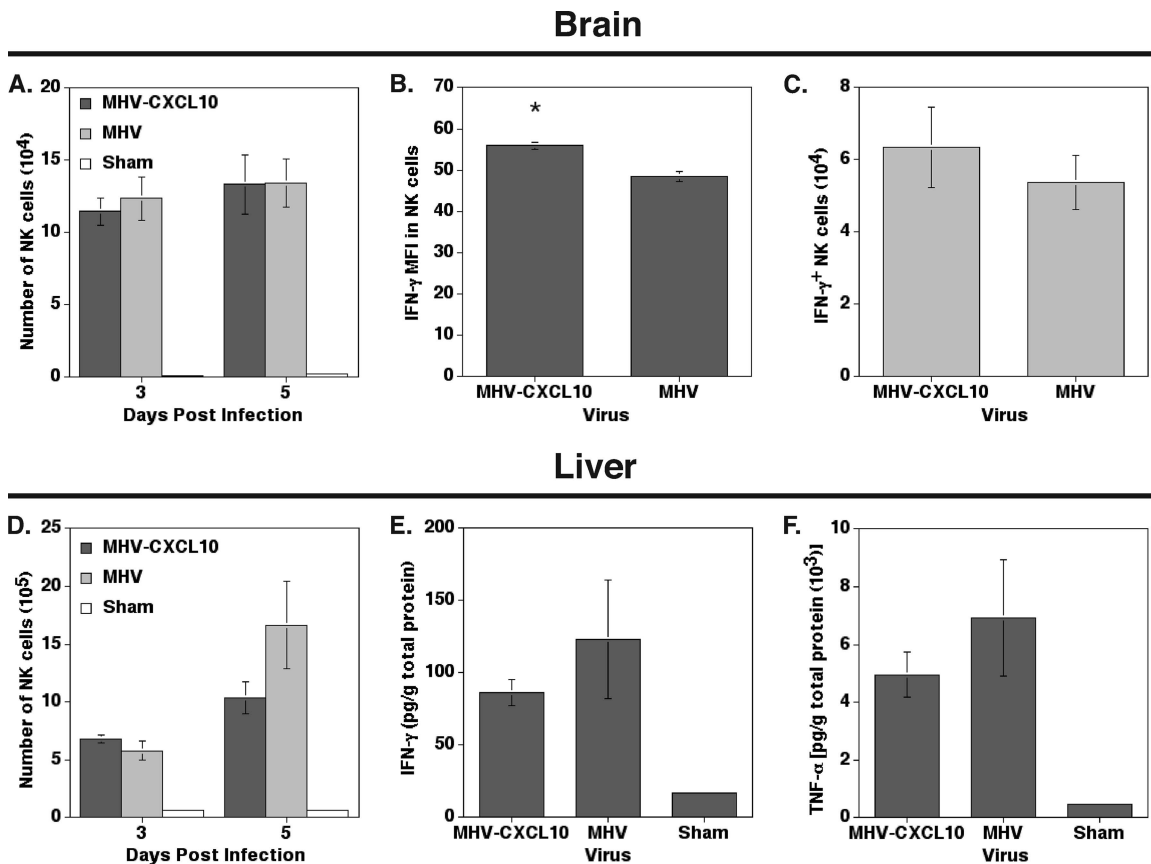


FIG. 3. NK cell infiltration into infected tissues was not affected by CXCL10 expression from the viral genome. (A) Infection with MHV-CXCL10 did not affect the total numbers of NK cells infiltrating into the brain at days 3 and 5 p.i. compared to the numbers for MHV-infected mice. (B) NK cells were isolated from the brains of SCID mice infected with either MHV-CXCL10 or MHV at day 5 p.i., and IFN- γ production was determined by intracellular staining. *, $P \leq 0.05$. (C) NK cells from MHV-CXCL10-infected mice exhibited increased production of IFN- γ compared to that of MHV-infected mice as measured by MFI, although there was no difference in the total numbers of IFN- γ -positive NK cells between mice infected with either virus. (D) Total numbers of NK cells infiltrating into the liver at day 3 p.i. were comparable between MHV-CXCL10- and MHV-infected mice, whereas the numbers increased in MHV-infected mice at day 5 p.i. compared to those for MHV-CXCL10-infected mice. In addition, MHV-CXCL10- and MHV-infected mice expressed comparable levels of IFN- γ (E) and TNF- α (F) proteins in the liver at day 5 p.i. Data in panels A to D are derived from two independent experiments with a minimum of three mice per group; ELISA data (E and F) are representative of three independent experiments with a minimum of two mice/group. Data are presented as the means \pm standard errors of the means.

(Fig. 3D). The increase of NK cells infiltrating into the livers of MHV-infected mice most likely was due to the increase in viral titers in the animals at this time. These data indicate that the expression of CXCL10 enhances protection from brain and liver disease by limiting viral replication in a manner independent of NK cell infiltration.

In order to determine the mechanisms by which CXCL10 expression enhances survival without affecting NK cell infiltration, NK cell effector functions were analyzed. The expression of IFN- γ by infiltrating leukocytes is important for controlling MHV replication within the brain (30, 38). Intracellular staining for IFN- γ on NK cells revealed significantly increased ($P \leq 0.05$) IFN- γ levels in NK cells within the CNS of mice infected with MHV-CXCL10 compared to those of mice infected with MHV at day 5 p.i., although there were no significant differences between absolute numbers of NK cells expressing IFN- γ within the brains of mice infected with either virus (Fig. 3B and C). In addition, mice infected with either virus had similar amounts of IFN- γ and TNF- α protein present within the livers

at day 5 p.i., as determined by ELISA (Fig. 3E and F). These data demonstrate that MHV-CXCL10 infection results in enhanced IFN- γ secretion specifically in the brain but does not affect either IFN- γ or TNF- α production in the liver, highlighting organ-specific determinants for cytokine secretion.

Cytolytic activity by infiltrating NK cells also might be important in controlling viral replication in either the brains or liver. However, there was no difference in intracellular granzyme B expression in NK cells isolated from either the brains or the livers of mice infected with MHV-CXCL10 or MHV (data not shown). These findings suggest that CXCL10 expression from the MHV genome does not regulate factors associated with NK cell-mediated cytolytic function.

NKG2D ligands are expressed in brain and liver following viral infection. Enhanced IFN- γ secretion by NK cells within the brains of MHV-CXCL10-infected mice might result from the increased local expression of ligands capable of binding to NK cell-activating receptors such as NKG2D (8). Therefore, we next employed quantitative real-time PCR to evaluate

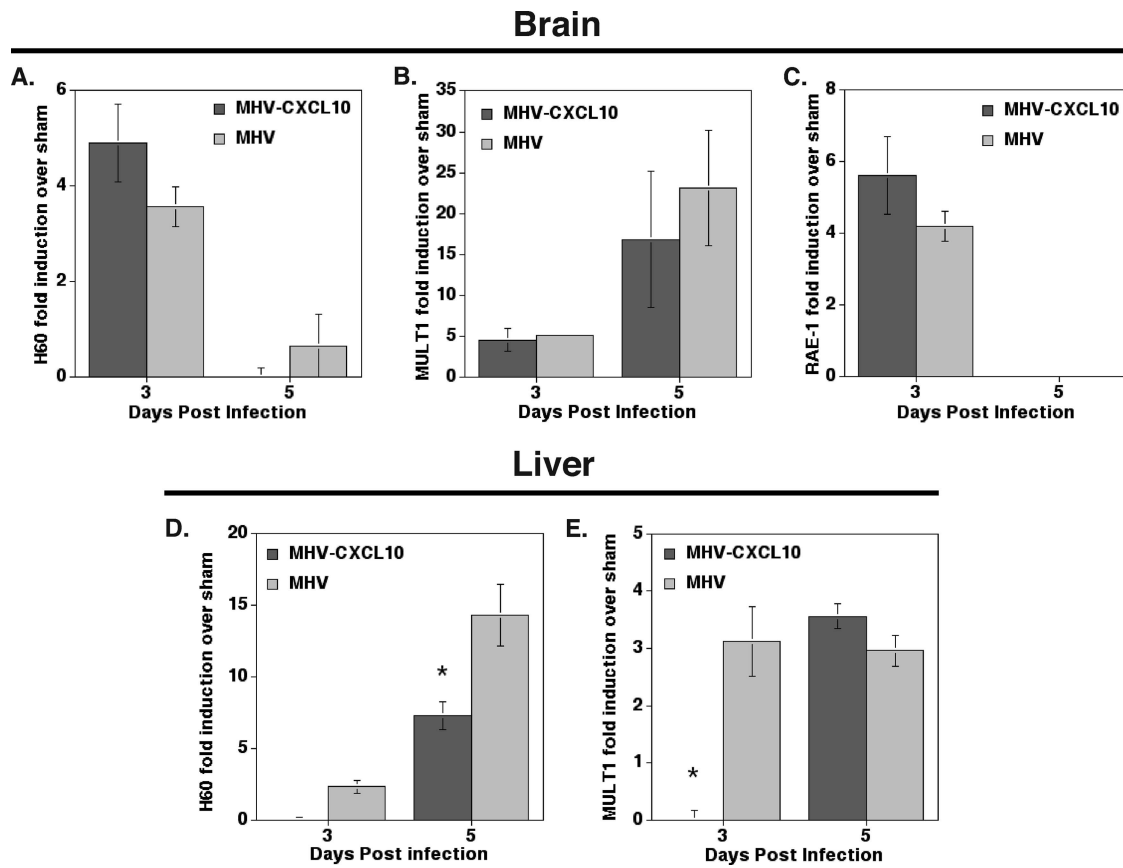


FIG. 4. NKG2D ligand mRNA expression. Infection of SCID mice with either MHV-CXCL10 or MHV results in increased expression of H60 (A), MULT1 (B), and RAE-1 (C) transcripts at day 3 p.i. within the brain compared to their expression in sham-infected mice. H60 and RAE-1 expression in MHV-CXCL10- and MHV-infected mice at day 5 p.i. was similar to those of sham-infected mice. (B) MULT1 mRNA expression was induced to a level 15-fold greater than that of sham-infected mice in both MHV-CXCL10- and MHV-infected mice at day 5 p.i. Quantitative real-time PCR analysis of infected livers revealed similar levels of H60 (D) and MULT1 (E) transcripts in MHV-CXCL10-infected mice compared to those of sham-infected mice at day 3 p.i. In contrast, transcripts were induced above sham-infected-mouse levels in MHV-infected mice at this time (D and E). (D) At day 5 p.i., a statistically significant (*, $P \leq 0.05$) decrease of H60 transcripts in MHV-CXCL10-infected livers compared to those of MHV-infected mice was observed. (E) However, MULT1 transcript levels were comparable between both experimental groups at day 5 p.i. RAE-1 was not increased above the level for sham-infected mice in either MHV-CXCL10- or MHV-infected mice at any time in the liver. A minimum of four mice from each experimental condition were used, and data are presented as the means \pm standard errors of the means.

mRNA transcripts for the NKG2D ligands H60, MULT1, and RAE-1 within the brain and liver in response to infection with either MHV-CXCL10 or MHV. The expression of both H60 and RAE-1 transcripts was induced transiently to levels greater than those of sham-infected mice only at day 3 p.i. in brains (Fig. 4A and C), whereas MULT1 transcripts were increased at both days 3 and 5 p.i. in the brains of infected mice (Fig. 4B). Elevated levels of transcripts for both H60 and MULT1 were detected in the livers of MHV-infected SCID mice at days 3 and 5 p.i., whereas transcripts for these ligands were induced above the levels for sham-infected mice at day 5 p.i. in the livers of MHV-CXCL10-infected mice (Fig. 4D and E). The levels of H60 transcripts in MHV-CXCL10-infected mice were decreased ($P \leq 0.05$) compared to the levels in MHV-infected mice at day 5 p.i. (Fig. 4D). In contrast to the findings for the brain, RAE-1 was not induced above the level of expression in sham-infected mice in the liver at any time point examined following infection with either virus, indicating the differential transcription of NKG2D ligands within virus-infected tissue (data not shown). Furthermore, these findings suggest that

CXCL10 does not modulate ligand expression within the brain, as no differences were noted between MHV-CXCL10- and MHV-infected mice, but CXCL10 might influence H60 and MULT1 transcription in the liver.

NKG2D is expressed on NK cells infiltrating the brain and liver following viral infection. The ability of CXCL10 to modulate NKG2D receptor expression on NK cells infiltrating into infected tissue was analyzed. The average numbers of NKG2D-positive NK cells were equivalent in the brains of mice infected with either MHV-CXCL10 or MHV at days 3 and 5 p.i. (Fig. 5A). In addition, there were no differences in the overall frequencies of NKG2D-positive NK cells, and the MFI of NKG2D on the surface of NK cells were equivalent between MHV-CXCL10- and MHV-infected mice within the brain at days 3 and 5 p.i. (not shown). Similarly, an examination of the livers of infected mice indicated no differences in numbers (Fig. 5B) and frequencies (not shown) of NKG2D-expressing infiltrating NK cells at day 3 p.i. (Fig. 5B). However, by day 5 p.i. there was an increase in the number of NKG2D-positive NK cells (Fig. 5B) and frequencies (not shown)

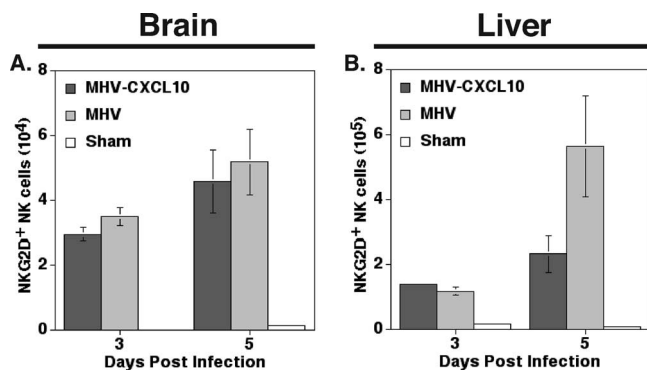


FIG. 5. NKG2D receptor is expressed on NK cells present within infected tissues. (A) The average numbers of NK cells expressing NKG2D in the brains of MHV-CXCL10- and MHV-infected mice at days 3 and 5 p.i. were equivalent. (B) In the liver, the average numbers of gated (DX5⁺, CD3⁻) NK cells expressing NKG2D are similar between the treatment groups at day 3 p.i. However, by day 5 p.i., there was an increase in the numbers of NKG2D-positive NK cells in MHV-infected mice, but this difference was not significant. Very few NK cells were detected in the brains or livers of sham-infected mice. Data are representative of two independent experiments with a minimum of four mice/group and are presented as the means \pm standard errors of the means.

present in MHV-infected mice compared to those for MHV-CXCL10-infected mice that correlated with an increase in numbers of NK cells present in the livers (Fig. 3D). An analysis of the MFI of NKG2D on NK cells infiltrating into the liver on days 3 and 5 p.i. indicates similar expression levels between MHV-CXCL10 and MHV infections (not shown).

Anti-NKG2D treatment does not influence disease. To further explore the possibility that NKG2D is important in amplifying NK cell responses that control viral replication and increase survival, mice were infected i.c. with MHV-CXCL10 and treated with a neutralizing, nondepleting anti-NKG2D MAb or a control rat IgG antibody. The administration of anti-NKG2D did not result in increased mortality compared to that for control-treated mice (Fig. 6A). Viral titers in the brains did not differ between experimental groups at any time assayed, but anti-NKG2D-treated mice exhibited a significant ($P \leq 0.05$) increase in viral burden in the liver at day 5 p.i. compared to that of mice treated with rat IgG (Fig. 6B). The average number of NK cells infiltrating into the brain was not affected by anti-NKG2D treatment (Fig. 6C). However, there was an increase in NK cells present within the livers of anti-NKG2D-treated mice at day 5 p.i., but the difference was not significant (Fig. 6D). An analysis of sALT levels determined that anti-NKG2D treatment did not enhance liver pathology in MHV-CXCL10-infected mice compared to that of control-treated mice (Fig. 6E). In addition, histological sections of livers from antibody-treated mice revealed no differences in the severity of hepatitis between treatment groups at day 5 p.i. (data not shown). Binding of the neutralizing anti-NKG2D antibody CX5 results in receptor internalization, thus compromising signaling through NKG2D (25, 29). Therefore, in order to confirm that the administration of anti-NKG2D to MHV-CXCL10-infected mice resulted in diminished NKG2D receptor expression, another anti-NKG2D MAb (MI-6) recognizing a different epitope of the receptor was used to quantitate the

amount of NKG2D surface expression on NK cells by flow cytometry (16). Mice were infected i.c. with MHV-CXCL10 and treated with rat IgG or anti-NKG2D CX5. MI-6 MAb staining demonstrated that anti-NKG2D CX5 MAb treatment decreased NKG2D surface expression on NK cells in all tissues analyzed at day 5 p.i., whereas treatment with control antibody did not diminish NKG2D staining (Fig. 6F). Therefore, injection of anti-NKG2D MAb CX5 resulted in NKG2D internalization on NK cells. The above-described data demonstrate that NKG2D signaling has little effect on neurological disease and host survival but reduces the viral burden in the liver without significantly affecting NK cell infiltration or liver pathology.

DISCUSSION

NK cells display a diverse array of unique surface receptors that employ various mechanisms to facilitate the recognition of virally infected cells and to elicit the activation of antiviral effector pathways. Among these is NKG2D, which is a lectin-like stimulatory receptor that originally was described to be important in tumor cell recognition and immunity (2, 8). However, NKG2D now is recognized to be important with regard to the regulation of lymphocyte responses in autoimmune diseases such as diabetes (28), colitis (15, 17), celiac disease (27), and rheumatoid arthritis (11) as well as to participate in host defense following viral infection (7, 9, 18, 23–25, 33, 34). Indeed, studies by Lodoen et al. and others have clearly demonstrated that NKG2D signaling on NK cells is critical for the control of the replication of MCMV lacking viral genes that can down-regulate the expression of RAE-1, H60 (24, 25), and MULT1 (18, 23). The secretion of IFN- γ by NK cells is mediated in part by NKG2D signaling (24). These findings have helped define signaling pathways used by NK cells that are important in controlling viral proliferation.

The present study was undertaken to extend our understanding of how localized expression of CXCL10 protects against virus-induced disease within the context of the innate immune response. We previously have reported that CXCL10 produced by the recombinant MHV-CXCL10 virus is protective following the infection of immunodeficient mice through the CXCL10-mediated attraction of NK cells into the CNS (38). Indeed, blocking CXCL10 signaling or depleting NK cells resulted in increased viral titers within the brain. The present study was undertaken to extend our understanding of the underlying mechanisms associated with CXCL10-mediated protection following viral infection. Specifically, we were interested to determine if CXCL10 signaling enhanced the expression of NKG2D ligands or the NKG2D receptor on NK cells, which in turn might result in NKG2D-mediated NK cell activation and the subsequent control of viral replication. Our findings argue against a protective role for NKG2D in NK cell protection from disease following MHV infection of immunodeficient BALB/c mice. Although elevated mRNA transcripts specific for the NKG2D ligands H60, MULT1, and RAE-1 were detected in both the brains and livers of MHV-CXCL10-infected mice, there were no overt differences between these mice and those infected with the isogenic control virus, MHV. Ligand transcript expression in the brains of mice infected with either virus indicated that levels of H60 and RAE-1 were

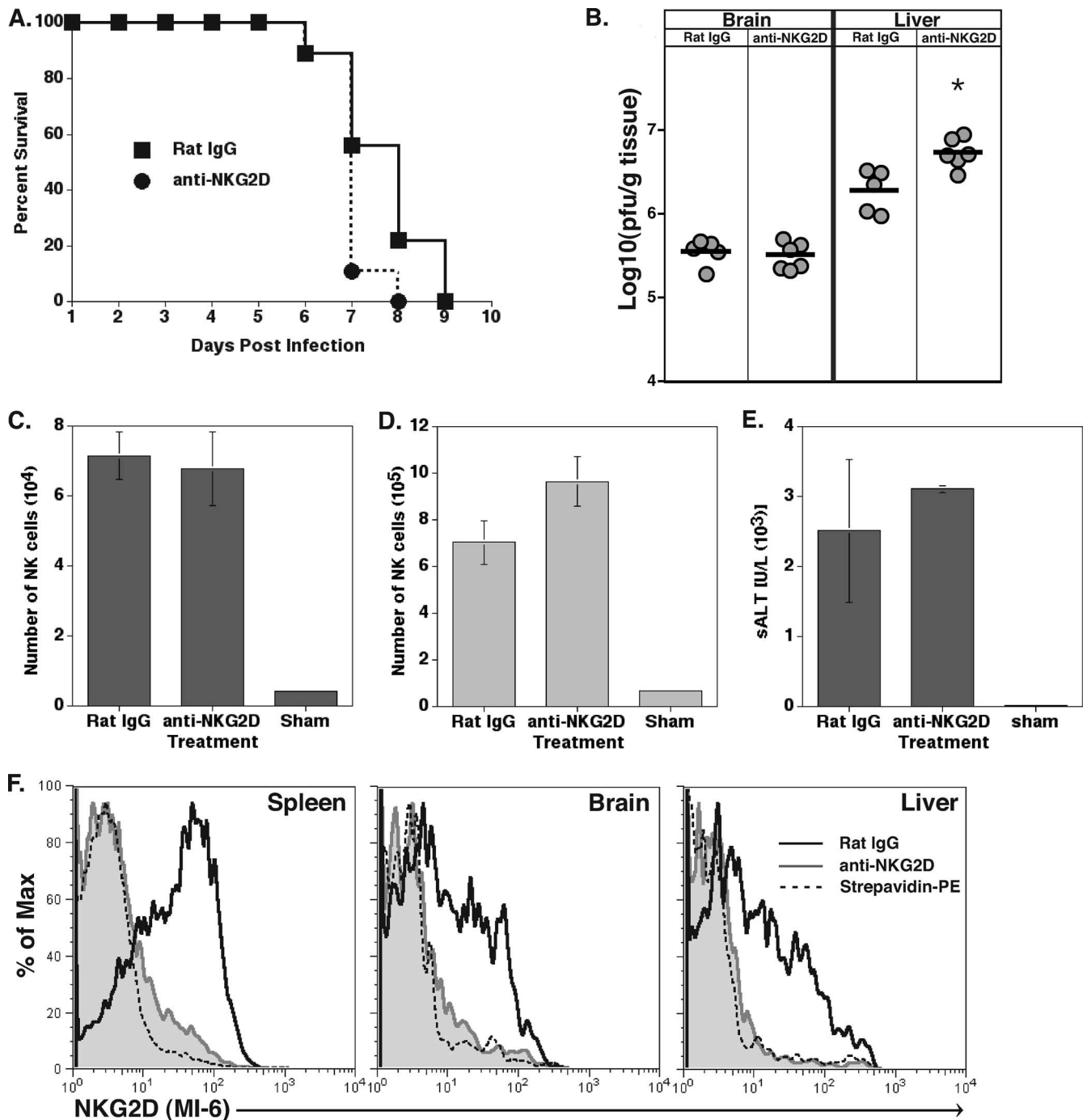


FIG. 6. NKG2D signaling has organ-specific functions. (A) NKG2D neutralization in MHV-CXCL10-infected mice resulted in a similar level of survival compared to that of mice treated with control antibody. (B) There were comparable levels of virus in the brains of rat IgG- and anti-NKG2D-treated mice at day 5 p.i. Anti-NKG2D-treated mice exhibited a statistically significant (*, $P \leq 0.05$) increase in the viral titer ($\sim 0.5 \log_{10}$ PFU/g tissue) in the liver compared to that of rat IgG-treated mice at day 5 p.i. NK cell infiltration was not affected in the brains (C) or livers (D) of anti-NKG2D-treated mice compared to that in tissues of control rat IgG-treated mice. Data are representative of two independent experiments with a minimum of four mice per group and are presented as the means \pm standard errors of the means. (E) Treatment with anti-NKG2D antibody did not affect sALT levels compared to treatment with the control rat IgG at day 5 p.i. sALT data are representative of two individual experiments with no fewer than three mice per treatment group. (F) Anti-NKG2D (gray-tinted line) treatment of MHV-CXCL10-infected mice resulted in decreased NKG2D cell surface expression (determined by staining with anti-NKG2D antibody MI-6) in the spleen, brain, and liver compared to the level of expression in rat IgG-treated mice (solid black line) at day 5 p.i. Cells treated with PE-conjugated streptavidin (black dashed line) were included as a negative control for comparison. Histograms are of representative mice from each treatment group.

elevated early but declined at later time points, suggesting a rapid and transient expression profile in response to viral infection. In contrast, MULT1 transcripts were expressed at comparatively lower levels at day 3 p.i. but increased by day 5, supporting the possibility that the local production of cytokines enhances MULT1 expression. In contrast, RAE-1 transcripts were not detected within the livers of virus-infected mice. CXCL10 may suppress H60 expression, because the levels of transcripts were comparatively diminished at all time points examined compared to those of MHV-infected mice. Although MULT1 transcript levels were diminished at day 3 p.i. in livers of MHV-CXCL10-infected mice compared to those of MHV-infected mice, there were no differences in transcript levels at day 5 p.i. Collectively, these findings highlight differences in the tissue-specific expression of NKG2D ligands in response to coronavirus infection and suggest the potential for the CXCL10-mediated regulation of expression. More importantly, the administration of an NKG2D-blocking antibody did not affect NK cell infiltration into the brain or liver, and there was no increase in viral replication in the brain. However, anti-NKG2D treatment of MHV-CXCL10-infected mice did result in a significant increase in viral burden within the liver, demonstrating a partial role for NKG2D signaling in protection against MHV-induced liver disease. This is similar to infection with MCMV deficient in genes able to block the expression of the NKG2D ligands on MCMV-infected cells, in which NKG2D signaling augments IFN- γ secretion by NK cells (24). The underlying mechanisms by which NKG2D stimulates a protective response in the livers of MHV-infected mice remain to be determined. Moreover, our data suggest that CXCL10 influences NK cell-mediated IFN- γ expression, as there was increased intracellular staining in NK cells present within the brains of MHV-CXCL10-infected mice compared to that for MHV-infected mice, yet there was no appreciable difference in NK cell accumulation in the CNS of the two treatment groups. However, we would caution against a general role for CXCL10 in amplifying antiviral effector responses, because we have recently determined that MHV infection of CXCL10-deficient mice does not result in deficient proliferation, trafficking, IFN- γ secretion, or cytolytic activity by virus-specific T cells (35).

In this study, we also determined that MHV-CXCL10 infection results in reduced liver pathology that is independent of NK cell infiltration and IFN- γ and TNF- α secretion. In addition, this protection did not rely on NKG2D signaling. Previously, we showed that CXCL10 expression from MHV-CXCL10 infection is hepatoprotective in CXCL10^{-/-} mice. The reduced pathology was not due to the modulation of cell infiltration, IFN- γ secretion, or hepatocyte prosurvival signaling through CXCR2 (41). In the present study, the amount of hepatocyte necrosis, the degree of portal inflammation, and especially the degree of lobular inflammation were different between treatment groups, with overall less severe pathology observed in MHV-CXCL10-infected mice than in mice infected with MHV. Other pathological parameters were not noticeably different. Importantly, there was not a unique difference in the type of response between mice infected with either MHV-CXCL10 or MHV, just a difference in the severity of disease, which likely relates to the reduction of viral titers within tissues of MHV-CXCL10-infected mice. Both experi-

mental groups showed hepatitis with primarily intra- and periportal inflammation as well as attendant necrosis. Taking the results together, these studies demonstrate that CXCL10 is hepatoprotective through a mechanism not dependent on T cells, NK cells, NKG2D signaling, CXCR2 signaling, or IFN- γ and TNF- α secretion, and it is still under investigation.

In conclusion, the findings put forth support and extend earlier studies demonstrating that CXCL10 amplifies the innate immune response to viral infection, as demonstrated by prolonged survival and reduced viral titers in infected organs (38). Additionally, the protective effect exerted by localized CXCL10 expression within the brain following MHV infection is not dependent upon NKG2D. In the liver, NKG2D only partially contributes to the control of MHV replication, although transcripts of the NKG2D ligands were clearly up-regulated by MHV infection in both brain and liver. These data illustrate that NKG2D signaling on NK cells does not represent a universally evoked antiviral effector host defense mechanism but that NK cells are capable of responding to different environmental stimuli to control viral replication in different tissue environments.

ACKNOWLEDGMENTS

We are indebted to Wenqiang Wei (University of Southern California, Los Angeles, CA) for tissue processing and staining.

National Institutes of Health grants NS41249 to T.E.L. and AI066897 to L.L.L. supported this work. A Pilot Research Award from the National Multiple Sclerosis Society to T.E.L. also supported this work. L.L.L. is an American Cancer Society Research Professor.

L.L.L. and the University of California (San Francisco, CA) have licensed intellectual property rights relative to NKG2D for commercial applications.

REFERENCES

- Agresti, A. 1992. A survey of exact interference for contingency tables. *Stat. Sci.* 7:131-177.
- Bauer, S., V. Groh, J. Wu, A. Steinle, J. H. Phillips, L. L. Lanier, and T. Spies. 1999. Activation of NK cells and T cells by NKG2D, a receptor for stress-inducible MICA. *Science* 285:727-729.
- Bergmann, C. C., B. Parra, D. R. Hinton, R. Chandran, M. Morrison, and S. A. Stohlman. 2003. Perforin-mediated effector function within the central nervous system requires IFN-gamma-mediated MHC up-regulation. *J. Immunol.* 170:3204-3213.
- Cerwenka, A., A. B. Bakker, T. McClanahan, J. Wagner, J. Wu, J. H. Phillips, and L. L. Lanier. 2000. Retinoic acid early inducible genes define a ligand family for the activating NKG2D receptor in mice. *Immunity* 12:721-727.
- Cerwenka, A., J. L. Baron, and L. L. Lanier. 2001. Ectopic expression of retinoic acid early inducible-1 gene (RAE-1) permits natural killer cell-mediated rejection of a MHC class I-bearing tumor in vivo. *Proc. Natl. Acad. Sci. USA* 98:11521-11526.
- Cook, D. N., M. A. Beck, T. M. Coffman, S. L. Kirby, J. F. Sheridan, I. B. Pragnell, and O. Smithies. 1995. Requirement of MIP-1 alpha for an inflammatory response to viral infection. *Science* 269:1583-1585.
- Dandekar, A. A., K. O'Malley, and S. Perlman. 2005. Important roles for gamma interferon and NKG2D in $\gamma\delta$ T-cell-induced demyelination in T-cell receptor β -deficient mice infected with a coronavirus. *J. Virol.* 79:9388-9396.
- Diefenbach, A., A. M. Jamieson, S. D. Liu, N. Shastri, and D. H. Raulet. 2000. Ligands for the murine NKG2D receptor: expression by tumor cells and activation of NK cells and macrophages. *Nat. Immunol.* 1:119-126.
- Dunn, C., N. J. Chalupny, C. L. Sutherland, S. Dosch, P. V. Sivakumar, D. C. Johnson, and D. Cosman. 2003. Human cytomegalovirus glycoprotein UL16 causes intracellular sequestration of NKG2D ligands, protecting against natural killer cell cytotoxicity. *J. Exp. Med.* 197:1427-1439.
- Ebers, G. C., D. E. Bulman, A. D. Sadovnick, D. W. Paty, S. Warren, W. Hader, T. J. Murray, T. P. Seland, P. Duquette, T. Grey, et al. 1986. A population-based study of multiple sclerosis in twins. *N. Engl. J. Med.* 315:1638-1642.
- Groh, V., A. Bruhl, H. El-Gabalawy, J. L. Nelson, and T. Spies. 2003. Stimulation of T cell autoreactivity by anomalous expression of NKG2D and its MIC ligands in rheumatoid arthritis. *Proc. Natl. Acad. Sci. USA* 100:9452-9457.

12. Groh, V., R. Rhinehart, J. Randolph-Habecker, M. S. Topp, S. R. Riddell, and T. Spies. 2001. Costimulation of CD8 $\alpha\beta$ T cells by NKG2D via engagement by MIC induced on virus-infected cells. *Nat. Immunol.* **2**:255–260.
13. Hamerman, J. A., K. Ogasawara, and L. L. Lanier. 2004. Cutting edge: Toll-like receptor signaling in macrophages induces ligands for the NKG2D receptor. *J. Immunol.* **172**:2001–2005.
14. Hirano, N., T. Murakami, K. Fujiwara, and M. Matsumoto. 1978. Utility of mouse cell line DBT for propagation and assay of mouse hepatitis virus. *Jpn. J. Exp. Med.* **48**:71–75.
15. Ito, Y., T. Kanai, T. Totsuka, R. Okamoto, K. Tsuchiya, Y. Nemoto, A. Yoshioka, T. Tomita, T. Nagaishi, N. Sakamoto, T. Sakanishi, K. Okumura, H. Yagita, and M. Watanabe. 2008. Blockade of NKG2D signaling prevents the development of murine CD4⁺ T cell-mediated colitis. *Am. J. Physiol. Gastrointest. Liver Physiol.* **294**:199–207.
16. Jamieson, A. M., A. Diefenbach, C. W. McMahon, N. Xiong, J. R. Carlyle, and D. H. Raulet. 2002. The role of the NKG2D immunoreceptor in immune cell activation and natural killing. *Immunity* **17**:19–29.
17. Kjellek, S., C. Haase, D. Lundsgaard, B. Urso, D. Tornehave, and H. Markholst. 2007. Inhibition of NKG2D receptor function by antibody therapy attenuates transfer-induced colitis in SCID mice. *Eur. J. Immunol.* **37**:1397–1406.
18. Krmpotic, A., M. Hasan, A. Loewendorf, T. Saulig, A. Halenius, T. Lenac, B. Polic, I. Bubic, A. Kriegeskorte, E. Pernjak-Pugel, M. Messerle, H. Hengel, D. H. Busch, U. H. Koszinowski, and S. Jonjic. 2005. NK cell activation through the NKG2D ligand MULT-1 is selectively prevented by the glycoprotein encoded by mouse cytomegalovirus gene m145. *J. Exp. Med.* **201**:211–220.
19. Lane, T. E., V. C. Asensio, N. Yu, A. D. Paoletti, I. L. Campbell, and M. J. Buchmeier. 1998. Dynamic regulation of alpha- and beta-chemokine expression in the central nervous system during mouse hepatitis virus-induced demyelinating disease. *J. Immunol.* **160**:970–978.
20. Lane, T. E., M. T. Liu, B. P. Chen, V. C. Asensio, R. M. Samawi, A. D. Paoletti, I. L. Campbell, S. L. Kunkel, H. S. Fox, and M. J. Buchmeier. 2000. A central role for CD4⁺ T cells and RANTES in virus-induced central nervous system inflammation and demyelination. *J. Virol.* **74**:1415–1424.
21. Langsrud, Ø., K. Jørgensen, R. Ragni Ofstad, and T. Næs. 2007. Analyzing designed experiments with multiple responses. *J. Appl. Stat.* **34**:1275–1296.
22. Lavi, E., D. H. Gilden, M. K. Highkin, and S. R. Weiss. 1986. The organ tropism of mouse hepatitis virus A59 in mice is dependent on dose and route of inoculation. *Lab. Anim. Sci.* **36**:130–135.
23. Lenac, T., M. Budt, J. Arapovic, M. Hasan, A. Zimmermann, H. Simic, A. Krmpotic, M. Messerle, Z. Ruzsics, U. H. Koszinowski, H. Hengel, and S. Jonjic. 2006. The herpesviral Fc receptor fcr-1 down-regulates the NKG2D ligands MULT-1 and H60. *J. Exp. Med.* **203**:1843–1850.
24. Lodoen, M., K. Ogasawara, J. A. Hamerman, H. Arase, J. P. Houchins, E. S. Mocarski, and L. L. Lanier. 2003. NKG2D-mediated natural killer cell protection against cytomegalovirus is impaired by viral gp40 modulation of retinoic acid early inducible 1 gene molecules. *J. Exp. Med.* **197**:1245–1253.
25. Lodoen, M. B., G. Abenes, S. Umamoto, J. P. Houchins, F. Liu, and L. L. Lanier. 2004. The cytomegalovirus m155 gene product subverts natural killer cell antiviral protection by disruption of H60-NKG2D interactions. *J. Exp. Med.* **200**:1075–1081.
26. Luster, A. D., and P. Leder. 1993. IP-10, a -C-X-C- chemokine, elicits a potent thymus-dependent antitumor response in vivo. *J. Exp. Med.* **178**:1057–1065.
27. Meresse, B., Z. Chen, C. Ciszewski, M. Tretiakova, G. Bhagat, T. N. Krausz, D. H. Raulet, L. L. Lanier, V. Groh, T. Spies, E. C. Ebert, P. H. Green, and B. Jabri. 2004. Coordinated induction by IL15 of a TCR-independent NKG2D signaling pathway converts CTL into lymphokine-activated killer cells in celiac disease. *Immunity* **21**:357–366.
28. Ogasawara, K., J. A. Hamerman, L. R. Ehrlich, H. Bour-Jordan, P. Santamaria, J. A. Bluestone, and L. L. Lanier. 2004. NKG2D blockade prevents autoimmune diabetes in NOD mice. *Immunity* **20**:757–767.
29. Ogasawara, K., J. A. Hamerman, H. Hsin, S. Chikuma, H. Bour-Jordan, T. Chen, T. Pertel, C. Carnaud, J. A. Bluestone, and L. L. Lanier. 2003. Impairment of NK cell function by NKG2D modulation in NOD mice. *Immunity* **18**:41–51.
30. Parra, B., D. R. Hinton, N. W. Marten, C. C. Bergmann, M. T. Lin, C. S. Yang, and S. A. Stohman. 1999. IFN-gamma is required for viral clearance from central nervous system oligodendroglia. *J. Immunol.* **162**:1641–1647.
31. Pfaffl, M. W. 2001. A new mathematical model for relative quantification in real-time RT-PCR. *Nucleic Acids Res.* **29**:e45.
32. Qin, S., J. B. Rottman, P. Myers, N. Kassam, M. Weinblatt, M. Loetscher, A. E. Koch, B. Moser, and C. R. Mackay. 1998. The chemokine receptors CXCR3 and CCR5 mark subsets of T cells associated with certain inflammatory reactions. *J. Clin. Investig.* **101**:746–754.
33. Röfle, A., M. Mousavi-Jazi, M. Eriksson, J. Odeberg, C. Soderberg-Naucler, D. Cosman, K. Karre, and C. Cerboni. 2003. Effects of human cytomegalovirus infection on ligands for the activating NKG2D receptor of NK cells: up-regulation of UL16-binding protein (ULBP)1 and ULBP2 is counteracted by the viral UL16 protein. *J. Immunol.* **171**:902–908.
34. Sirén, J., T. Sareneva, J. Pirhonen, M. Strengell, V. Veckman, I. Julkunen, and S. Matikainen. 2004. Cytokine and contact-dependent activation of natural killer cells by influenza A or Sendai virus-infected macrophages. *J. Gen. Virol.* **85**:2357–2364.
35. Stiles, L. N., J. L. Hardison, C. S. Schaumburg, L. M. Whitman, and T. E. Lane. 2006. T cell antiviral effector function is not dependent on CXCL10 following murine coronavirus infection. *J. Immunol.* **177**:8372–8380.
36. Taub, D. D., A. R. Lloyd, K. Conlon, J. M. Wang, J. R. Ortaldo, A. Harada, K. Matsushima, D. J. Kelvin, and J. J. Oppenheim. 1993. Recombinant human interferon-inducible protein 10 is a chemoattractant for human monocytes and T lymphocytes and promotes T cell adhesion to endothelial cells. *J. Exp. Med.* **177**:1809–1814.
37. Taub, D. D., D. L. Longo, and W. J. Murphy. 1996. Human interferon-inducible protein-10 induces mononuclear cell infiltration in mice and promotes the migration of human T lymphocytes into the peripheral tissues and human peripheral blood lymphocytes-SCID mice. *Blood* **87**:1423–1431.
38. Trifilo, M. J., C. Montalto-Morrison, L. N. Stiles, K. R. Hurst, J. L. Hardison, J. E. Manning, P. S. Masters, and T. E. Lane. 2004. CXC chemokine ligand 10 controls viral infection in the central nervous system: evidence for a role in innate immune response through recruitment and activation of natural killer cells. *J. Virol.* **78**:585–594.
39. Turner, R. B. 1988. Rhinovirus infection of human embryonic lung fibroblasts induces the production of a chemoattractant for polymorphonuclear leukocytes. *J. Infect. Dis.* **157**:346–350.
40. Van Damme, J., B. Decock, R. Conings, J. P. Lenaerts, G. Opendakker, and A. Billiau. 1989. The chemotactic activity for granulocytes produced by virally infected fibroblasts is identical to monocyte-derived interleukin 8. *Eur. J. Immunol.* **19**:1189–1194.
41. Walsh, K. B., R. A. Edwards, K. M. Romero, M. V. Kotlajich, S. A. Stohman, and T. E. Lane. 2007. Expression of CXC chemokine ligand 10 from the mouse hepatitis virus genome results in protection from viral-induced neurological and liver disease. *J. Immunol.* **179**:1155–1165.
42. Xie, J. H., N. Nomura, M. Lu, S. L. Chen, G. E. Koch, Y. Weng, R. Rosa, J. Di Salvo, J. Mudgett, L. B. Peterson, L. S. Wicker, and J. A. DeMartino. 2003. Antibody-mediated blockade of the CXCR3 chemokine receptor results in diminished recruitment of T helper 1 cells into sites of inflammation. *J. Leukoc. Biol.* **73**:771–780.